Am J Transl Res 2017;9(10):4481-4491
www.ajtr.org /ISSN:1943-8141/AJTR0054131

Original Article

Feasibility of magnetic resonance redox imaging at low magnetic field: comparison at 1 T and 7 T

Mizuki Nakamura[1,4*], Sayaka Shibata[2], Toshihide Yamasaki[5**], Megumi Ueno[1], Ikuo Nakanishi[1], Ken-ichiro Matsumoto[1], Tadashi Kamada[3,4], Ken-ichi Yamada[5,6], Ichio Aoki[2]

[1]Quantitative RedOx Sensing Team, Department of Basic Medical Sciences for Radiation Damages, National Institute of Radiological Sciences, National Institutes for Quantum and Radiological Science and Technology, 4-9-1 Anagawa, Inage-ku, Chiba 263-8555, Japan; [2]Functional and Molecular Imaging Team, Department of Molecular Imaging and Theranostics, National Institute of Radiological Sciences, National Institutes for Quantum and Radiological Science and Technology, 4-9-1 Anagawa, Inage-ku, Chiba 263-8555, Japan; [3]Clinical Research Cluster, National Institute of Radiological Sciences, National Institutes for Quantum and Radiological Science and Technology, 4-9-1 Anagawa, Inage-ku, Chiba 263-8555, Japan; [4]Graduate School of Medical and Pharmaceutical Sciences, Chiba University, 1-8-1 Inohana, Chuo-ku, Chiba 260-88670, Japan; [5]Department of Bio-functional Science, Faculty of Pharmaceutical Sciences, Kyushu University, 3-1-1 Maidashi, Higashi-ku, Fukuoka 812-8582, Japan; [6]JST, PRESTO, 4-1-8 Honcho, Kawaguchi, Saitama 332-0012, Japan; [*]Present address: Department of Radiology, Kitasato University Hospital, 1-15-1 Kitasato, Minami-ku, Sagamihara-shi, Kanagawa 252-0375, Japan; [**]Present address: Biophysical Chemistry, Kobe Pharmaceutical University, 4-19-1 Motoyamakita, Higashinada, Kobe, Hyogo 658-8558, Japan

Received March 29, 2017; Accepted July 12, 2017; Epub October 15, 2017; Published October 30, 2017

Abstract: The effect of different static magnetic field strengths, 1 T or 7 T, on the quality of nitroxyl radical-based magnetic resonance redox imaging (MRRI) was examined. A stable nitroxyl radical, 3-methoxycarbonyl-2,2,5,5-tetramethylpyrrolidine-*N*-oxyl (MC-PROXYL), was used as a T_1 contrast agent. Phantoms and animals were scanned at 1 T and 7 T using a similar gradient echo sequence. The quality of T_1-weighted images and susceptibility of T_1-weighted signals were compared. The nitroxyl radical-based T_1-weighted signal enhancement ratio was higher at 1 T compared with at 7 T when the identical phantom was scanned using a similar gradient echo sequence. The gradient echo scanning at 7 T was sensitive to movement and/or flux of the sample solution, which could result in the distortion of baseline T_1-weighted signals. No such wobbling of the signal was observed when the experiment was done at 1 T. The detection at the lower field is less affected by voltex flow in the sample, much stable T_1-weighted signal detection is available at the lower field. The visual characteristics of *in vivo* nitroxyl decay profiles were similar between the 1 T and 7 T experiments, except noises were large at 1 T. The correlation trends of *in vivo* decay constants among brain regions also similar between 1 T and 7 T experiments. Nitroxyl radical-based MRRI could be an adequate theranostic tool when performed on clinically popular low magnetic field MRI instruments.

Keywords: Redox-sensitive contrast agent, magnetic resonance imaging, nitroxyl radical, T_1-weighted contrast, gradient echo, signal decay rate

Introduction

To provide safe and efficient radiation therapy, the observation of patho-physiological information from diseased tissue is very important. Oxygen concentration and/or redox status in target tissues, which can affect prognosis, is beneficial information for planning radiation therapy. Noninvasive imaging techniques to provide such bio-functional information have been developed on magnetic resonance based imaging modalities, such as electron paramagnetic resonance imaging (EPRI), magnetic resonance imaging (MRI), and Overhauser MRI (OMRI; also known as proton-electron double resonance imaging [PEDRI]).

The redox imaging technique, which can estimate tissue redox status non-invasively, utilizes nitroxyl radicals as a redox-sensitive contrast agent. Nitroxyl radicals are stable free radical species; however, nitroxyl radicals can be enzy-

Table 1. Physical, chemical, and biological properties of MC-PROXYL

Chemical Name	3-methoxycarbonyl-2,2,5,5-tetramethylpyrrolidine-*N*-oxyl	
Chemical Formula	$C_{10}H_{18}NO_3$	
Structure	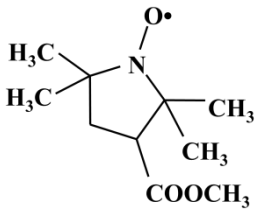	
Molecular Weight	200	
Appearance	Yellow blown liquid	
Water Solubility	150 mmol/L or more	
Toxicity	1.5 μmol/g b.w., bolus *i.v.*	Trappy
	0.75 μmol/g b.w., bolus i.v.	Safe
Biological Property	Blood-brain-barrier permeable amphiphilic molecule	

matically reduced to their corresponding hydroxyl amines in living cells. The *in vivo* reduction rate of the nitroxyl radical was changed in pathological redox conditions. Numerous pathophysiological cases changing *in vivo* redox states were reported by electron paramagnetic resonance (EPR; also known as electron spin resonance [ESR]) spectroscopic experiments [1-12]. For example, inflammation models in rat stomach mucosa [1, 2], which providehydroxyl radicals and/or superoxides, can accelerate the nitroxyl reduction rate, or the Se-deficient rat model [3], which generates hydrogen peroxide-rich conditions, decreased the nitroxyl reduction rate. It was reported using 3-methoxycarbonyl-2,2,5,5-tetramethylpyrrolidine-*N*-oxyl (MC-PROXYL), a blood-brain-barrier permeable amphiphilic nitroxyl radical, as a redox probe that X-irradiation to mouse whole body modified tissue redox status and make the reduction rate slower [4].

The redox imaging technique was initially developed in the field of EPR [13, 14]. EPR can directly detect paramagnetic species through the absorption of microwave and/or radio frequencies by the electron spins existing in a magnetic field. EPR can be combined with magnetic resonance based imaging to map stable paramagnetic compounds, such as nitroxyl radicals [15-17]. Several studies of *in vivo* EPRI, including pioneering work on redox imaging, were reported in the late 1990s [18-24]. EPRI, however, has some problems that need to be overcome, including low spatial resolution, low temporal resolution, no anatomical information, and volume limitation of the subject.

From the middle 2000s, MRI-based high-resolution redox imaging techniques have been reported [25]. MRI can also detect nitroxyl radicals thorough proton-T_1 shortening effects of the paramagnetism of nitroxyl radicals. In other words, nitroxyl radicals can give contrast enhancement on T_1-weighted MR images. By utilizing MRI to detect nitroxyl radicals, most of difficulties associated with EPRI were resolved. In addition, MRI has become a widely used diagnostic tool in clinical use, although the most-popular clinical MRI instruments work at relatively low field strengths of <3 T. However, most animal experiments were done at higher field strengths >4.7 T to obtain higher signal-to-noise ratios (SNR) and resulting higher spatial resolution [25-27]. In addition to the clinical systems, several low field preclinical MRI systems using 1 T permanent magnet have been developed and improved for in vivo measurements. In general, T_1-contrast agents show higher T_1-relaxivity at lower magnetic field [28].

High field instruments can give increasing SNR, which can be a significant advantage on the image based diagnosis. In homogeneity of RF field associated with high field operation requires proper shimming, which lead a technical complexity and difficulty of manipulation. In addition, high field magnetic resonance requires corresponding higher frequency and RF power, which makes specific absorption ratio (SAR) larger. Low field instruments face the issue of lower SNR; however, can provide much easy manipulating, human-body-friendly and wallet-friendly diagnostics. Especially for redox imaging, which is a kind of dynamic imaging and requires sequence of scans, low field instruments, which can keep SAR lower, may be suitable, when the redox information can be obtained adequately. Therefore, in this paper, the basic features of 1 T and 7 T MRI on nitroxyl-induced contrast were compared to consider the feasibility of redox imaging at low magnetic field strengths.

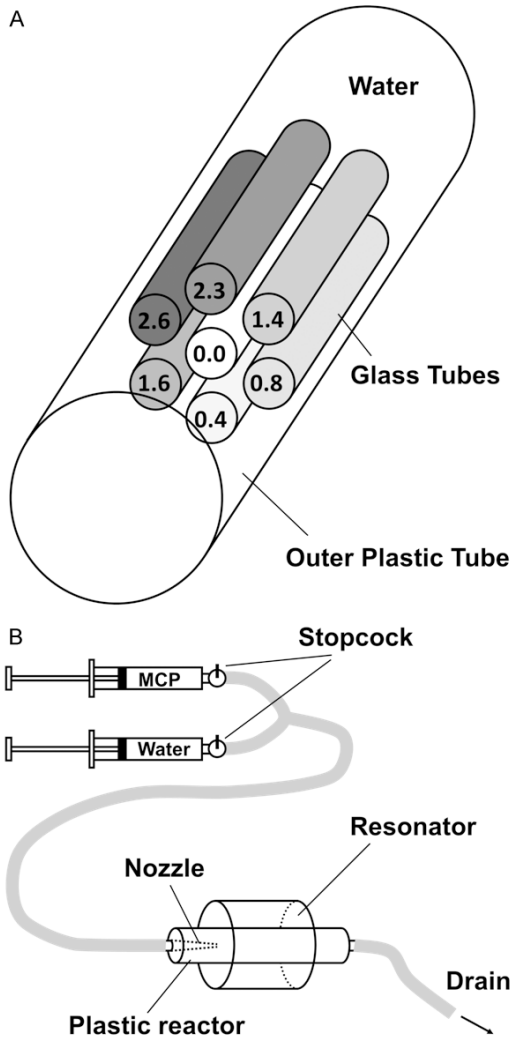

Figure 1. Schematic drawing of the phantoms. A: Phantom-1: seven hexagonally arranged glass tubes (i.d. = 6.4 mm, o.d. = 8.0 mm), containing different concentrations of MC-PROXYL-water solutions, were immersed in a larger outer plastic tube (Falcon, 50 mL disposable centrifuge tube) filled with pure water. Numbers in the figure are the concentrations of the MC-PROXYL in mM. B: Phantom-2: syringes containing the same volume of 4 mmol/L MC-PROXYL water solution or pure water were connected to a single plastic cylindrical reactor (internal diameter, 12.7 mm) through bifurcated vinyl tubing. The reactor and the connected lines were filled with pure water. The solutions in the syringes were pushed out, delivered into the reactor via the vinyl tubing, and then entered through a nozzle, which caused an unstable vortex water flow in the reactor. Surplus volume from reaction mixture was drained.

Materials and methods

Chemicals

3-Methoxycarbonyl-2,2,5,5-tetramethylpyrrolidine-*N*-oxyl (MC-PROXYL) was synthesized in accordance with the method reported previously [22, 29]. The physical, chemical, and biological properties of MC-PROXYL are arranged in **Table 1**. Deionized water (Milli-Q system, Merck Millipore, Billerica, MA, USA) was used for preparing MC-PROXYL water solutions.

Animals

Seven-week-old female C3H mice were supplied by Japan SLC, Inc. (Shizuoka, Japan) Animals were housed five per cage in climate-controlled (23 ± 1°C and 55 ± 5% humidity), circadian rhythm-adjusted (12-hr light-dark cycle) rooms and were allowed food and water *ad libitum*. Mice were used for experiments after a habituation period of 1 week. Experiments were carried out in compliance with and approved by the Animal Use Committee of the National Institute of Radiological Sciences.

Phantoms

Phantom-1 was composed of seven glass tubes (i.d. = 6.4 mm, o.d. = 8.0 mm) filled with 0, 0.4, 0.8, 1.4, 1.6, 2.3, 2.6 mM water solutions of MC-PROXYL, a nitroxyl contrast agent. The hexagonally arranged glass tubes were immersed in a larger outer plastic tube (Falcon, 50 mL disposal centrifuging tube) filled with pure water. The arrangement of phantom-1 is shown in **Figure 1A**.

Phantom-2 (**Figure 1B**) was designed to observe the stability of image intensity, which can be disturbed vortexes flowing in a liquid sample. Syringes containing the same volume of 4 mmol/L MC-PROXYL water solution or pure water were connected to a single plastic cylindrical reactor (i.d. = 12.7 mm, length = 55 mm) through bifurcated vinyl tubing. The reactor and the connected lines were filled with pure water. When both syringes were pressed at the same time and at the same rate, the solutions in the syringes mixed through the vinyl tubing, and then delivered into the reactor through a nozzle, which produced an unstable vortex water flow in the reactor. Surplus volume from the reaction mixture was drained.

MRI scanner and pulse sequences

MR images were acquired using a 7 T horizontal MRI scanner (Magnet: 40 cm bore, Kobelco and Jastec, Kobe, Japan; console and electronics: Avence-I system and ParaVision® 5.1 sys-

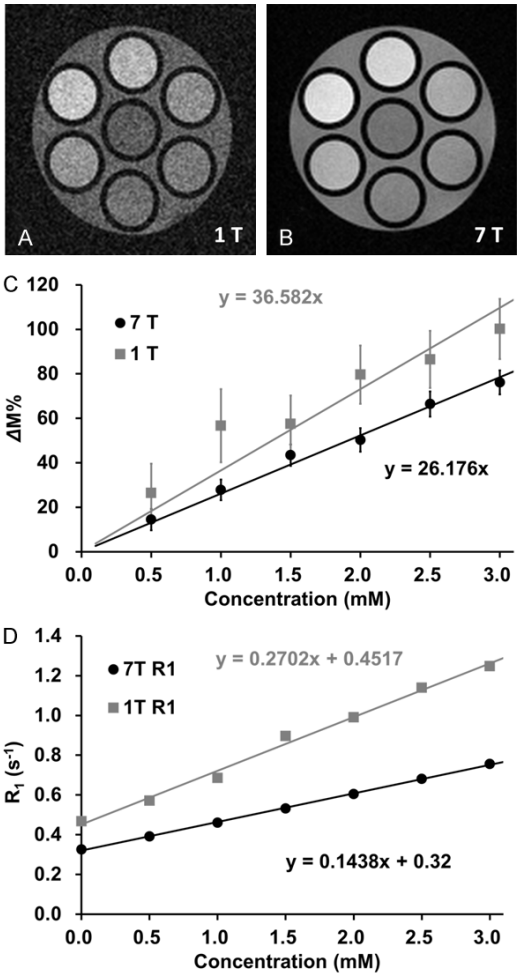

Figure 2. Comparison of T_1-weighted images of phantom-1 scanned by FLASH (TE = 5.1 ms, TR = 75 ms, FA = 45°) at 1 T and 7 T. T_1-weighted MR images obtained at (A) 1 T and (B) 7 T. (C) Relations of percentage signal amplification (ΔM%) and concentrations of MC-PROXYL obtained at 1 T and 7 T. (D) Relations of T_1-relaxivity (R_1) and concentrations of MC-PROXYL obtained at 1 T and 7 T.

tem, BrukerBiospin, Ettlingen, Germany) and 1 T horizontal MRI scanner (permanent magnet, ParaVision® 5.1 system, BrukerBiospin). For *in vitro* 7 T MRI acquisition, a 35-mm inner-diameter quadrature volume coil for transmission and reception (Rapid Biomedical, Rimpar, Germany) was used. Sample temperature was maintained at room temperature (23 ± 0.5°C) using a gradient cooling system and air-conditioner. For *in vitro* 1 T MRI acquisition, a 35-mm inner-diameter solenoid coil (6-turned) for transmission and reception (Aspect Imaging, Shoham, Israel) was used. Sample temperature was maintained at room temperature (23 ± 0.5°C) using a fan and air-conditioner. For phantom-1, 2-dimensional, single-slice, inversion-recovery MRI was performed using a rapid acquisition with relaxation enhancement (RARE) sequence with the following parameters for T_1 relaxometry: repetition time (TR) = 10,000 ms, effective echo time (TE) = 20 ms, inversion time = 52, 75, 100, 200, 400, 800, 1600, 3200, and 6400 ms, matrix size = 128 × 128, FOV = 32 × 32 mm, slice thickness (ST) = 2 mm, and number of acquisitions (NA) = 1. The slice orientation was horizontal. The total acquisition time was 5 min 20 s. For phantom-2, a set of five slices (0.75 mm thick with 0.75 mm gaps) of T_1-weighted images was obtained repeatedly 70 times by multi slice FLASH sequences using the following parameters: TE = 6 ms (for 1 T) or 5.1 ms (for 7 T), TR = 75 ms, FA = 45°, matrix size = 128 × 128, FOV = 25.6 × 25.6 mm, and NA = 2. The nominal voxel resolution was 200 × 200 μm. The acquisition time for one set was 19.2 s, and the total scan time was 22 min 24 s.

For *in vivo* 7 T MRI acquisition, MR images were obtained using a same 7 T MRI scanner (40 cm bore, Kobelco + Jastec, and BrukerBiospin) witha 72-mm inner-diameter volume coil for transmission (BrukerBiospin) and a quadrature surface coil for reception (mouse head, Rapid Biomedical, Rimpar, Germany). Rectal temperature was maintained at 36 ± 0.5°C using a heater (Raid Biomedical). For *in vivo* 1 T MRI acquisition, MR images were obtained using a same 1 T MRI scanner (BrukerBiospin) with a 6-turned solenoid coil (Aspect Imaging). Rectal temperature was maintained at 36 ± 0.5°C using a warm-water circulation system. For both 7 T and 1 T *in vivo* MRI, same imaging parameters were used as *in vitro* phantom-2 study. All of the MRI data were reconstructed and analyzed using ParaVision software (Ver. 5.1, BrukerBiospin).

MRI measurement for phantoms

Phantom-1 was set on a MRI probe (volume coil for 7 T or solenoid coil for 1 T), and then scanned using multislice FLASH sequences, as described above. A single frame with five slices, which was vertical to the glass tubes, was obtained. For phantom-2, the plastic cylindrical reactor was set in the center of the MRI probe. A dynamic data set composed on 70 frames was obtained using multislice FLASH sequences. Frames were obtained every 20 s. Each frame contained five slices (1.5 mm thick with 2.5 mm center-to-center gap). After the 5th

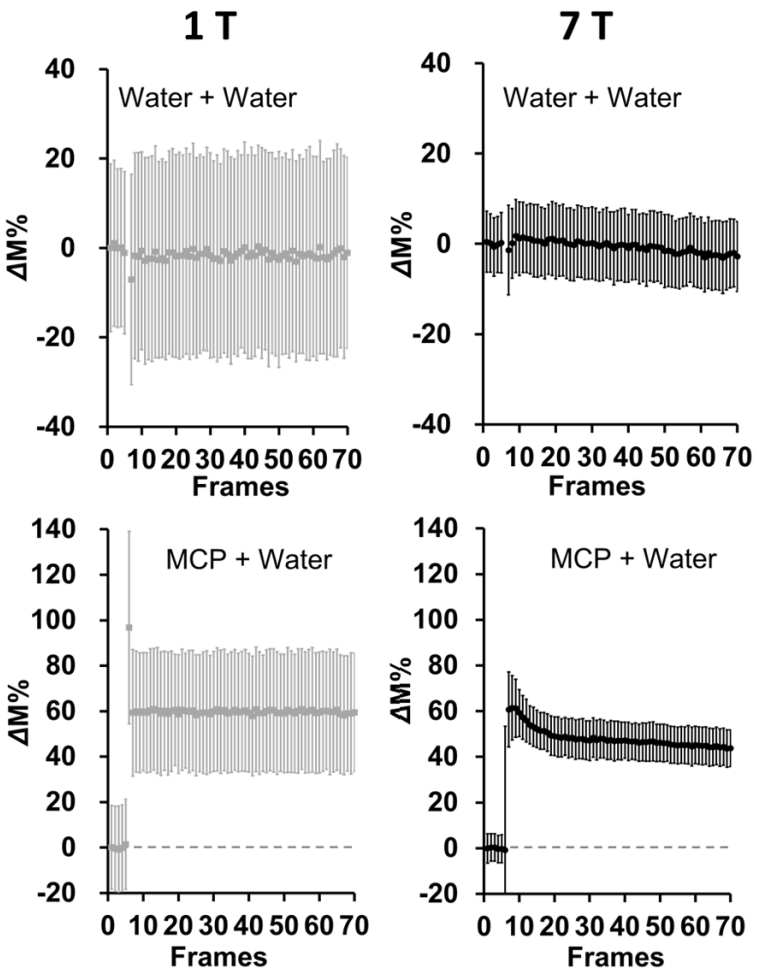

Figure 3. Comparison of T_1-signal stability observed using phantom-2 at 1 T and 7 T. Left and right panels are time courses of MC-PROXYL-induced T_1-weighted signals observed at 1 T and 7 T, respectively. Seventy frames were obtained every 20 sec. Two syringes connected to phantom-2 were pushed simultaneously, and the reaction mixtures were injected into the cylindrical reactor during the 6th frame and taking 10 sec. The upper panels show the results with water only, i.e. both syringes were filled with water. The lower panels show the result of mixing MC-PROXYL and water. Marks and error bars indicate average ΔM% values and standard deviation (SD) in a circular region of interest (ROI) set on the 3rd (center) slice of the five slices.

flame (i.e. from 1 min 40 s after the start of the scanning), both syringes were pushed at the same time and same rate to expel the reaction mixture. The injection took approximately 10 s. The scanning continued for further 20 min.

MRI measurement for an animal

A mouse was anesthetized using 2.0% isoflurane, and the tail vein was cannulated using a 30-gauge needle attached to a polyethylene tube (PE10, Becton Dickinson and Company, Sparks, MD, USA) for administration of MC-PROXYL. The mouse was placed on a body cradle (Rapid Biomedical) and immobilized using adhesive tape. The mouse was then placed in a proton volume radio-frequency (RF) resonator (72 mm i.d., BrukerBioSpin) with surface RF receiver (Rapid Biomedical). Rectal temperature was monitored using an optical fiber thermometer (FOT-M and FTI-10, FISO Technologies, Quebec, Canada) and electric temperature controller (E5CN, Omron, Kyoto, Japan) during MRI measurements. Breathing rate was monitored using a monitoring and gating system (Model 1030, SAII, New York, USA), and anesthesia was adjusted by watching the breathing rate on a case-by-case basis.

After 5th baseline image (1 min 40 sec), a 0.75 μmol/g b.w. (5 μL/g b.w. of 150 mM solution) of MC-PROXYL was injected intravenously. The injection, which took approximately 10 sec, was started at the beginning of the 6th scan and finished by the middle of 6th scan. The scanning continued for a further 20 min.

Image data analysis

MRI data were analyzed using ImageJ (a public domain Java image processing program that can be extended using plug-ins, http://rsb.info.nih.gov/ij/, NIH, Bethesda, MD, USA).

For dynamic imaging data, the T_1-weighted signal enhancement of a given pixel at (x, y) coordination, $\Delta M\%_{x,y}$, is as follows:

$$\triangle M\%_{x,y} = \left(\frac{S_{x,y} \text{ after CA injection}}{S_{x,y} \text{ before CA injection}} - 1\right) \times 100 \quad (1)$$

Where $S_{x,y}$ is the image intensity of a pixel (x, y). CA indicate "contrast agent" used in the experiment. "$S_{x,y}$ before CA injection" is an average image intensity of frame 1 to 5.

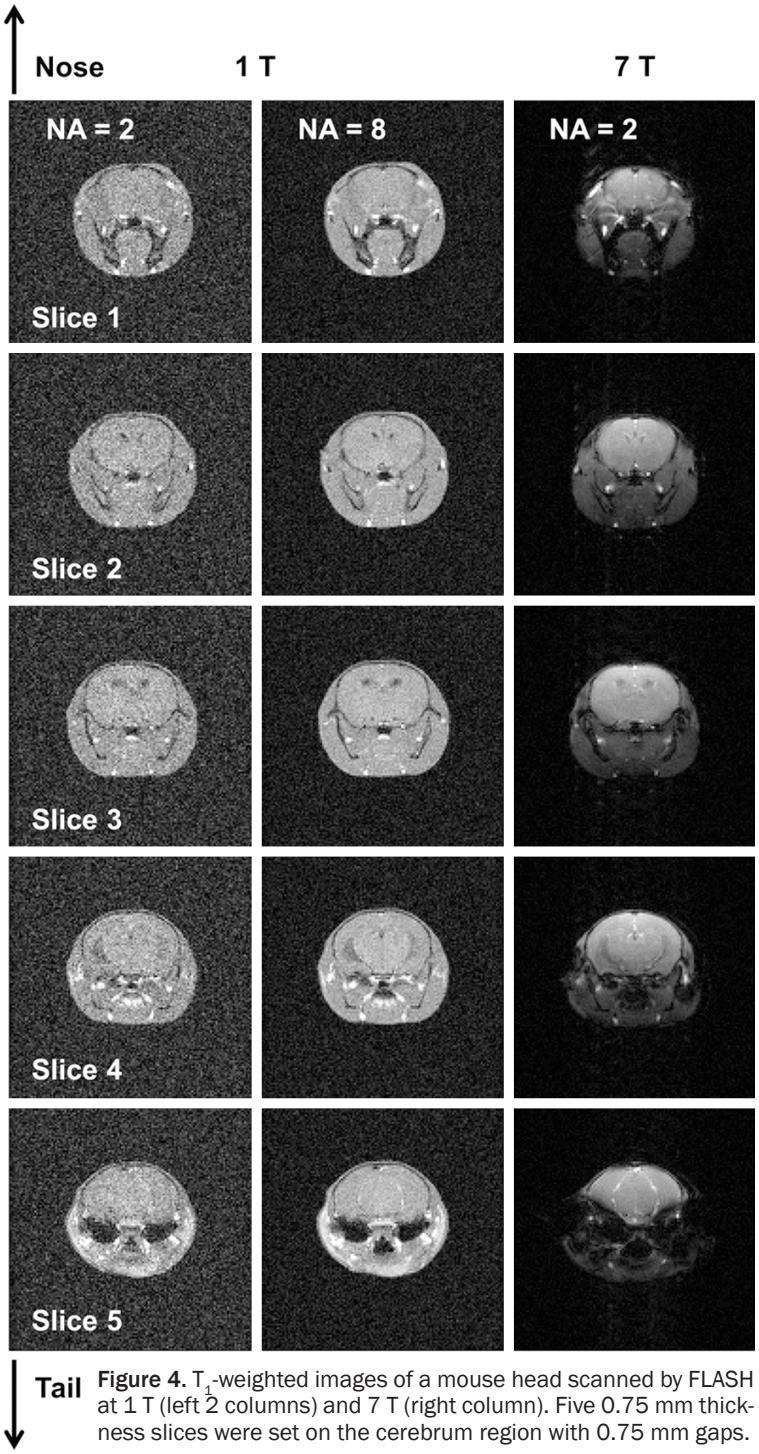

Figure 4. T_1-weighted images of a mouse head scanned by FLASH at 1 T (left 2 columns) and 7 T (right column). Five 0.75 mm thickness slices were set on the cerebrum region with 0.75 mm gaps.

L-band EPR measurement for an animal

A mouse was anesthetized using 1.5% isoflurane, and the tail vein was cannulated for injection of MC-PROXYL. The mouse was fixed on an acrylic holder, and placed in the gap of magnet pole pieces of the L-band EPR apparatus (JEOL, Tokyo Japan). The 1.1 GHz single loop surface coil (5.5 mm i.d.) was put on the parietal region of the mouse's head. The core body temperature in the rectum was monitored using a nonmagnetic probe (FISO Technologies Inc.), and was regulated at 37 ± 1°C using hot air and an infra-red lamp during EPR experiments. Immediately after the injection of the sterilized solution of MC-PROXYL into the tail vein (1.5 μmol/g b.w.), the lowest-field line of the triplet EPR spectra of MC-PROXYL in the head were measured repeatedly. The EPR conditions were as follows: microwave frequency = 1.04 GHz, scan rate = 10 mT/min, time constant = 0.1 sec, and field modulation frequency = 100 kHz, microwave power = 4.0 mW, and field modulation width = 1 mT. EPR data acquisition was controlled by the WIN-RAD ESR Data Analyzer System (Radical Research, Inc., Hino, Tokyo). The acquired EPR spectra were analyzed using an in-house line fitting program, and Gaussian line shape was fitted. The signal height and the line width of the fitted Gaussian line was measured and then EPR signal intensity was obtained by (signal height) × (line width)^2. The EPR signal decay constants, k_1 and k_2, of MC-PROXYL were calculated from the slope of the signal decay curves, which were determined from semi-logarithmic plots of the EPR signal intensity.

Results and discussion

An absolutely identical phantom sample was scanned using different MR scanners, one operated at 1 T and the other at 7 T. The resolution, or perhaps it should be said SNR, of the image scanned by the 1 T scanner (**Figure 2A**)

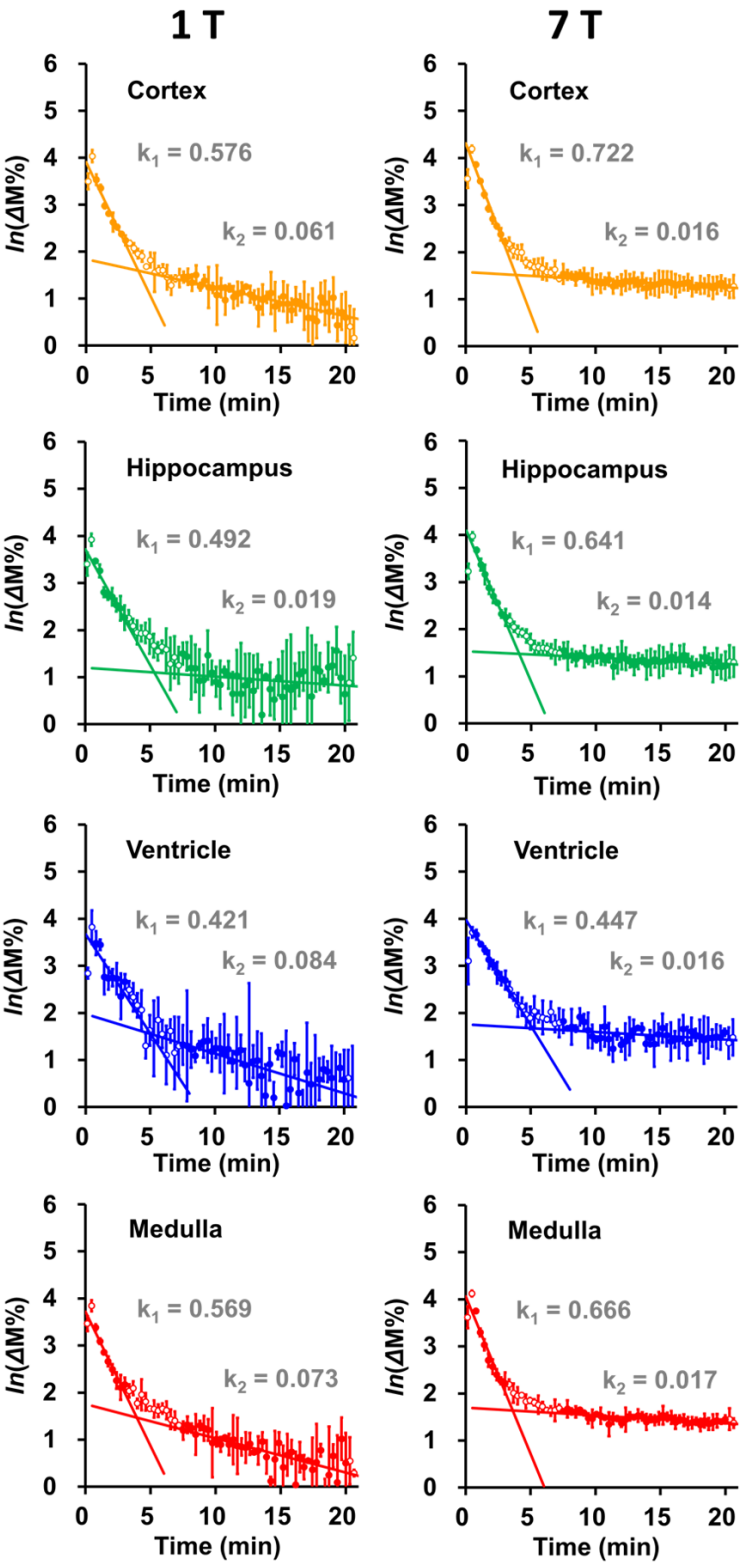

Figure 5. Comparison of decay profiles of MC-PROXYL-induced T_1-weighted signals in several brain areas of a mouse. Left and right columns showed the decay profiles obtained at 1 T and 7 T, respectively. Four regions of interest (ROIs), i.e. cortex, hippocampus, ventricle, and medulla areas, were set on the corresponding 5 slices of scout scan. Average ln (ΔM%) values were obtained for every brain areas. Finally, average ln (ΔM%) ± standard deviation (SD) of 3 mice was plotted versus time. The time window for calculating k_1 and k_2 was 0.8-3.0 min and 7.5-20.0 min, respectively.

was discernibly worse compared with that of the 7 T scanner (**Figure 2B**). Both 1 T and 7 T imaging conditions, however, could clearly show the 0.8 mm wall of the glass tubes. This may be enough resolution for distinguishing the anatomical structure in a large subject, such as human, monkey, and/or relatively large rodents.

Both 1 T and 7 T images (**Figure 2A** and **2B**, respectively) showed T_1-weighted contrast differences depending on the concentration of MC-PROXYL in the glass tubes. The region of interest (ROI) was set inside each glass tube. An average intensity value in the center tube, which contained water, was obtained as the baseline value. To digitize the percentage contrast enhancement induced by MC-PROXYL in the phantom-1 experiment, ΔM%, all pixel values were divided by the baseline value, subtract 1, and then multiply 100. An average value of ΔM% and SD in each ROI was recalculated and plotted versus the concentration of MC-PROXYL (**Figure 2C**). The T_1-weighted signal enhancement ratio, ΔM%, was larger at 1 T compared with at 7 T (**Figure 2C**). T_1-relaxivity values of MC-PROXYL evaluated from the data observed at 1 T and 7 T were 0.270 and 0.144 $mM^{-1}s^{-1}$, respectively (**Figure 2D**).

Figure 3 shows the results of the signal susceptibility test using phantom-2. The time courses of ΔM% images were

Table 2. Comparison of *in vivo* decay rates of MC-PROXYL obtained by 1 T or 7 T MRI

Brain Aria	k_1 (min^{-1})		k_2 (min^{-1})	
	1 T	7 T	1 T	7 T
Cortex	0.576 ± 0.024	0.722 ± 0.032*	0.061 ± 0.024	0.016 ± 0.006
Hippocampus	0.492 ± 0.078	0.641 ± 0.005	0.019 ± 0.017	0.014 ± 0.008
Ventricle	0.421 ± 0.223	0.447 ± 0.031	0.084 ± 0.018	0.016 ± 0.027*
Medulla	0.569 ± 0.056	0.666 ± 0.069	0.073± 0.018	0.017 ± 0.006*

n = 3. The time window for calculating k_1 and k_2 was 0.8-3.0 min and 7.5-20.0 min, respectively. *indicates significance between 1 T and 7 T by $p < 0.05$.

obtained as described in "*Image Data Analysis*." A circular ROI was placed on the inside area of the cylindrical reactor (image not shown), and an average ΔM% value and SD in the ROI was calculated for every slice of each frames. Five slices were observed for each frame. The results observed for only slice-3 (the center slice of five slices) are shown in **Figure 3**. The upper panels in **Figure 3** show the result with just flowing water, i.e. both syringes were filled with water and simply pressed simultaneously to make a vortex flow in the reactor. The lower panels show the results of mixing MC-PROXYL and water. The results obtained at 1 T and 7 T are shown in the left and right panels, respectively. The variation in values, SD error bar, appear larger at 1 T; however, the values were drifting almost horizontally (**Figure 3** left panels). The result obtained at 7 T showed less variation, but the values drifted forming a slight decay (**Figure 3** right panels). These results suggested that image intensity obtained at 1 T scanning was much more stable against flow patterns in the sample. These results also gave cause for concern regarding baseline fluctuation with 7 T scanning.

Figure 4 shows T_1-weighted images of a mouse head scanned before injecting MC-PROXYL. Distinguishing the anatomical structure in the mouse brain was more difficult in T_1-weighted images obtained at 1 T when NA was 2, although some details were discernible (left column). Lager NA (= 8) can give better anatomical details, even though the scans were done at 1 T (center column). The T_1-weighted images obtained at 7 T showed brain internal structures very clearly (right column), even when the NA was 2. For a mouse or a similar small subject, experiments using the 1 T imager may require extra processing to obtain high resolution exploratory images for estimating anatomical structures clearly.

Figure 5 shows the average decay profiles of T_1-weighted signals induced by MC-PROXYL in mouse brain regions. ROIs were put on the cortex, hippocampus, ventricle, and medulla area of the brain. The time course of *ln* (ΔM%) was plotted. The decay profiles of MC-PROXYL in each part of the brain showed basically two phases, i.e. an initial fast decay phase and a later slow decay phase. The initial fast decay reflected redox status in the tissue, and the later slow decay mostly reflected clearance [30, 31]. The estimated decay constants of the initial fast decay phase, k_1, showed a similar pattern in both the 1 T and 7 T experiments, where the k_1 decay rates of MC-PROXYL were quite rapid in the cortex and medulla compared with lower k_1 in the ventricle (**Table 2**). However, the estimated k_1 decay rates were slight faster in the 7 T experiments compared with the 1 T experiments (**Table 2**). This slight faster k_1 at 7 T may be due to unsteady baseline as shown in **Figure 3**. On the other hand, the estimated decay constants of the later slow phase, k_2, were slightly faster in the 1 T experiments compared with the 7 T experiments but were within an order of magnitude.

The L-band EPR experiment also showed a similar two-phase signal decay profile (data not shown), although the *in vivo* L-band EPR experiment was much suffered from a problem related to the broad fluctuation noises on the base line. The k_1 and k_2 values could be estimated as 0.504 ± 0.017 and 0.062 ± 0.045 min^{-1}, respectively. The L-band EPR experiment using surface coil, which probably reflects comprehensive EPR signal decay in the brain cortex, skull bone, and skin regions, is only as a guide, but showed similar values as that obtained for the cortex in the 1 T MRI experiments.

From the published pharmacokinetic results, the blood clearance rate of a membrane-impermeable hydrophilic triarylmethyl-type paramagnetic probe (Oxo63) in C3H mouse can be expected as 0.03-0.04 min^{-1} [32]. In addition, the k_2 decay rates of several nitroxyl probes

have been obtained as 0.06 min^{-1} or faster for C3H mouse [30] and as 0.055 min^{-1} or faster for Wistar rat [31]. Based on those previous data, the average k_2 values evaluated by the L-band EPR (0.062 min^{-1}) and the 1 T MRI experiments except hippocampus (0.061-0.084 min^{-1}) in this paper were, therefore, acceptable as the true physiological values. However, the k_2 value obtained as 0.019 min^{-1} in the hippocampus by 1 T experiment was viscerally too slow to accept as a natural physiological value. Relatively large noise in 1 T experiment may sometimes make such coincidental error. On the other hand, something certain artificial error can be suspected as a cause of relatively smaller k_2 values (0.014-0.017) evaluated by low noise 7 T MRI experiment in this paper.

Although higher noise levels in the 1 T instrument and lower signal stability in the 7 T instrument was obtained in *in vitro* experiments, both instruments could suitably estimate difference of the *in vivo* signal decay rate constants among different tissues/organs. Clinically popular lower field, i.e. 0.5-3.5 T, MRI instruments are inherently ready for utilization of redox imaging techniques, when a suitable clinically available redox-sensitive contrast agent becomes available. Development of a non-toxic redox-sensitive contrast agent is keenly awaited.

Conclusion

Nitroxyl radical-based redox imaging showed a satisfactory performance profile in a low magnetic field strength. Lower field, i.e. 1 T, MRI apparatus proposed higher T_1-relaxivity, even though the signal to noise ratio is lower, compare to higher field, i.e. 7 T, apparatus. In addition, the detection at the lower field is less affected by voltex flow in a sample, and then much stable T_1-weighted signal detection is available at the lower field. Although the shapes of *in vivo* nitroxyl decay curves and trends of *in vivo* nitroxyl decay constants among brain regions were similar between the 1 T and 7 T experiments, the decay constant values observed at 1 T experiment were rather as acceptable.

Acknowledgements

The authors are grateful to Yoshikazu Ozawa and Nobuhiro Nitta for their help with the MRI operation. This work was partly supported by JSPS KAKENHI Grant Numbers 24390011 and 26461901 (K. M.). This work was partially supported by JSPS KAKENHI Grant Number 16H01363 (K. Y.), by PRESTO from Japan Science and Technology Agency (K. Y.), and by the Platform Project for Supporting in Drug Discovery and Life Science Research from AMED, Japan, (K. Y.).

Disclosure of conflict of interest

None.

Address correspondence to: Dr. Ken-ichiro Matsumoto, Quantitative RedOx Sensing Team, Department of Basic Medical Sciences for Radiation Damages, National Institute of Radiological Sciences, National Institutes for Quantum and Radiological Science and Technology, 4-9-1 Anagawa, Inage-ku, Chiba 263-8555, Japan. Tel: +81-43-206-3123; Fax: +81-43-255-6819; E-mail: matsumoto.kenichiro@qst.go.jp

References

[1] Yasukawa K, Kasazaki K, Hyodo F, Utsumi H. Non-invasive analysis of reactive oxygen species generated in rats with water immersion restraint-induced gastric lesions using in vivo electron spin resonance spectroscopy. Free Radic Res 2004; 38: 147-155.

[2] Utsumi H, Yasukawa K, Soeda T, Yamada K, Shigemi R, Yao T, Tsuneyoshi M. Noninvasive mapping of reactive oxygen species by in vivo electron spin resonance spectroscopy in indomethacin-induced gastric ulcers in rats. J Pharmacol Exp Ther 2006; 317: 228-235.

[3] Matsumoto K, Endo K, Utsumi H. *In vivo* electron spin resonance assessment of decay constant of nitroxyl radical in selenium-deficient rat. Biol Pharm Bull 2000; 23: 641-644.

[4] Miura Y, Anzai K, Urano S, Ozawa T. In vivo electron paramagnetic resonance studies on oxidative stress caused by X-irradiation in whole mice. Free Radic Biol Med 1997; 23: 533-540.

[5] Miura Y, Utsumi H, Hamada A. Effects of inspired oxygen concentration on in vivo redox reaction of nitroxide radicals in whole mice. Biochem Biophys Res Commun 1992; 182: 1108-1114.

[6] Inaba K, Nakashima T, Shima T, Mitsuyoshi H, Sakamoto Y, Okanoue T, Kashima K, Hashiba M, Nishikawa H, Watari H. Hepatic damage influences the decay of nitroxide radicals in mice--an in vivo ESR study. Free Radic Res 1997; 27: 37-43.

[7] Matsumoto S, Mori N, Tsuchihashi N, Ogata T, Lin Y, Yokoyama H, Ishida S. Enhancement of nitroxide-reducing activity in rats after chronic administration of vitamin E, vitamin C, and idebenone examined by an in vivo electron spin resonance technique. Magn Reson Med 1998; 40: 330-333.
[8] Leonard SS, Mowrey K, Pack D, Shi X, Castranova V, Kuppusamy P, Vallyathan V. In vivo bioassays of acute asbestosis and its correlation with ESR spectroscopy and imaging in redox status. Mol Cell Biochem 2002; 234-235: 369-377.
[9] Ilangovan G, Li H, Zweier JL, Kuppusamy P. In vivo measurement of tumor redox environment using EPR spectroscopy. Mol Cell Biochem 2002; 234-235: 393-398.
[10] Takeshita K, Saito K, Ueda J, Anzai K, Ozawa T. Kinetic study on ESR signal decay of nitroxyl radicals, potent redox probes for in vivo ESR spectroscopy, caused by reactive oxygen species. Biochim Biophys Acta 2002; 1573: 156-164.
[11] Elas M, Parasca A, Grdina DJ, Halpern HJ. Oral administration is as effective as intraperitoneal administration of amifostine in decreasing nitroxide EPR signal decay in vivo. Biochim Biophys Acta 2003; 1637: 151-155.
[12] Swartz HM, Khan N, Khramtsov VV. Use of electron paramagnetic resonance spectroscopy to evaluate the redox state in vivo. Antioxid Redox Signal 2007; 9: 1757-1771.
[13] Kuppusamy P, Li H, Ilangovan G, Cardounel AJ, Zweier JL, Yamada K, Krishna MC, Mitchell JB. Noninvasive imaging of tumor redox status and its modification by tissue glutathione levels. Cancer Res 2002; 62: 307-312.
[14] Yamada KI, Kuppusamy P, English S, Yoo J, Irie A, Subramanian S, Mitchell JB, Krishna MC. Feasibility and assessment of non-invasive in vivo redox status using electron paramagnetic resonance imaging. Acta Radiol 2002; 43: 433-440.
[15] Alecci M, Colacicchi S, Indovina PL, Momo F, Pavone P, Sotgiu A. Three-dimensional in vivo ESR imaging in rats. Magn Reson Imaging 1990; 8: 59-63.
[16] Takeshita K, Utsumi H, Hamada A. ESR measurement of radical clearance in lung of whole mouse. Biochem Biophys Res Commun 1991; 177: 874-880.
[17] Ishida S, Matsumoto S, Yokoyama H, Mori N, Kumashiro H, Tsuchihashi N, Ogata T, Yamada M, Ono M, Kitajima T, Kamada H, Yoshida E. An ESR-CT imaging of the head of a living rat receiving an administration of a nitroxide radical. Magn Reson Imaging 1992; 10: 109-114.
[18] Alecci M, Ferrari M, Quaresima V, Sotgiu A, Ursini CL. Simultaneous 280 MHz EPR imaging of rat organs during nitroxide free radical clearance. Biophys J 1994; 67: 1274-1279.
[19] Yokoyama H, Ogata T, Tsuchihashi N, Hiramatsu M, Mori N. A spatiotemporal study on the distribution of intraperitoneally injected nitroxide radical in the rat head using an in vivo ESR imaging system. Magn Reson Imaging 1996; 14: 559-563.
[20] Nicholson I, Foster MA, Robb FJ, Hutchison JM, Lurie DJ. In vivo imaging of nitroxide-free-radical clearance in the rat, using radiofrequency longitudinally detected ESR imaging. J Magn Reson B 1996; 113: 256-261.
[21] Yokoyama H, Itoh O, Ogata T, Obara H, Ohya-Nishiguchi H, Kamada H. Temporal brain imaging by a rapid scan ESR-CT system in rats receiving intraperitoneal injection of a methyl ester nitroxide radical. Magn Reson Imaging 1997; 15: 1079-1084.
[22] Sano H, Matsumoto K, Utsumi H. Synthesis and imaging of blood-brain-barrier permeable nitroxyl-probes for free radical reactions in brain of living mice. Biochem Mol Biol Int 1997; 42: 641-647.
[23] Kuppusamy P, Wang P, Shankar RA, Ma L, Trimble CE, Hsia CJ, Zweier JL. In vivo topical EPR spectroscopy and imaging of nitroxide free radicals and polynitroxyl-albumin. Magn Reson Med 1998; 40: 806-811.
[24] Yokoyama H, Lin Y, Itoh O, Ueda Y, Nakajima A, Ogata T, Sato T, Ohya-Nishiguchi H, Kamada H. EPR imaging for in vivo analysis of the half-life of a nitroxide radical in the hippocampus and cerebral cortex of rats after epileptic seizures. Free Radic Biol Med 1999; 27: 442-448.
[25] Matsumoto K, Hyodo F, Matsumoto A, Koretsky AP, Sowers AL, Mitchell JB, Krishna MC. High-resolution mapping of tumor redox status by magnetic resonance imaging using nitroxides as redox-sensitive contrast agents. Clin Cancer Res 2006; 12: 2455-2462.
[26] Hyodo F, Matsumoto K, Matsumoto A, Mitchell JB, Krishna MC. Probing the intracellular redox status of tumors with magnetic resonance imaging and redox-sensitive contrast agents. Clin Cancer Res 2006; 12: 2455-2462.
[27] Zhelev Z, Bakalova R, Aoki I, Matsumoto K, Gadjeva V, Anzai K, Kanno I. Nitroxyl radicals as low toxic spin-labels for non-invasive magnetic resonance imaging of blood-brain barrier permeability for conventional therapeutics. Chem Commun (Camb) 2009; 2009: 53-55.
[28] Rinck PA, Muller RN. Field strength and dose dependence of contrast enhancement by gadolinium-based MR contrast agents. Eur Radiol 1999; 9: 998-1004.
[29] Sano H, Naruse M, Matsumoto K, Oi T, Utsumi H. A new nitroxyl-probe with high retention in the brain and its application for brain imaging. Free Radic Biol Med 2000; 28: 959-969.

[30] Matsumoto K, Krishna MC, Mitchell JB. Novel pharmacokinetic measurement using electron paramagnetic resonance spectroscopy and simulation of in vivo decay of various nitroxyl spin probes in mouse blood. J Pharmacol Exp Ther 2004; 310: 1076-1083.

[31] Okajo A, Matsumoto K, Mitchell JB, Krishna MC, Endo K. Competition of nitroxyl contrast agents as an in vivo tissue redox probe: comparison of pharmacokinetics by the bile flow monitoring (BFM) and blood circulating monitoring (BCM) methods using X-band EPR and simulation of decay profiles. Magn Reson Med 2006; 56: 422-431.

[32] Matsumoto K, English S, Yoo J, Yamada K, Devasahayam N, Cook JA, Mitchell JB, Subramanian S, Krishna MC. Pharmacokinetics of triarylmethyl-type paramagnetic spin probe used in EPR oximetry. Magn Reson Med 2004; 52: 885-892.